Inorganic Chemistry

Article

pubs.acs.org/IC

Theoretical Insight into the Ambiguous Endohedral Metallofullerene Er_3C_{74}: Covalent Interactions among Three Lanthanide Atoms

Yi-Jun Guo,[†] Hong Zheng,[†] Tao Yang,[‡] Shigeru Nagase,[§] and Xiang Zhao*[,†]

[†]Institute for Chemical Physics & Department of Chemistry, School of Science, State Key Laboratory of Electrical Insulation and Power Equipment, Xi'an Jiaotong University, Xi'an 710049, China

[‡]Institute for Molecular Science, Okazaki 444-8585, Japan

[§]Fukui Institute for Fundamental Chemistry, Kyoto University, Kyoto 606-8103, Japan

Supporting Information

ABSTRACT: All of C_{74}-based endohedral metallofullerenes (EMFs) are found to be monometallofullerenes with the same $D_{3h}(14246)$-C_{74} cage so far. An opening question is whether other C_{74} cages could survive during the production of some novel C_{74}-EMFs. Theoretically, we studied the trimetallic endohedral fullerene Er_3C_{74}, the existence of which had been proven without any further characterizations. Two thermodynamically stable Er_3C_{74} isomers were obtained, both of which could be expressed as $Er_3@C_{74}$, meaning that previously synthesized Er_3C_{74} is indeed an endohedral trierbium fullerene. Besides the isomer with well-known $D_{3h}(14246)$-C_{74} cage which obeys isolated pentagon rule (IPR), another one possesses the $C_1(13771)$-C_{74} cage with two adjacent pentagons. Notably, it is the first time an endohedral metallofullerene containing the $C_1(13771)$-C_{74} cage has been reported. Frontier orbitals analysis, bonding analysis in terms of quantum theory of atoms-in-molecule (QTAIM) and Mayer bond order, together with two-dimensional maps of electron localization function (ELF) and Laplacian of electron density of $Er_3@D_{3h}(14246)$-C_{74} and $Er_3@C_1(13771)$-C_{74} show obvious covalent interactions not only between metallic atoms and carbon cage but also among three erbium atoms. Finally, simulated IR spectra of $Er_3@D_{3h}(14246)$-C_{74} and $Er_3@C_1(13771)$-C_{74} were simulated, which should be useful to distinguish those two isomers.

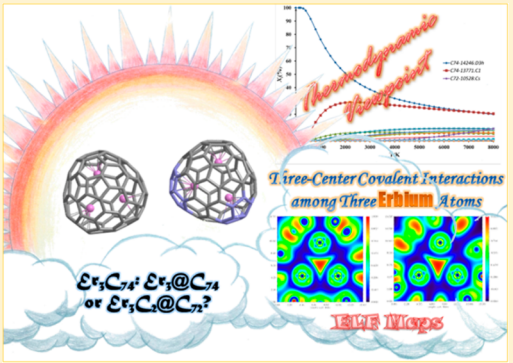

1. INTRODUCTION

After a few days of the discovery of the well-known buckminsterfullerene C_{60},[1] Smalley et al. have predicted that the "football" like structure contains a central cavity which should be an exceptionally strong binding site for a wide range of atoms or molecules.[2] Later, the prediction was confirmed, and this kind of novel molecule is called endohedral fullerene.[3] Among them, the most attractive species is endohedral metallofullerenes (EMFs). This is because of not only the special interactions between metal atoms and carbon ones,[4] but also varieties of potential applications in quantum computer,[5−7] photovoltaics,[8−10] and biomedicine.[11−13]

EMFs can be divided into conventional metallofullerenes and metal clusterfullerenes. Remarkably, it was long believed that the number of metal atoms forming a conventional metallofullerene is no more than two. In other words, when three or more metal atoms are encapsulated in a fullerene cage, doping with nonmetal atoms is a necessity, forming a series of metal clusterfullerenes. To date, some endohedral fullerenes of which inner clusters consist of as many as four metal atoms have been synthesized, such as $Sc_4O_2@C_{80}$,[14] $Sc_4O_3@C_{80}$,[15] and $Sc_4C_2@C_{80}$.[16] Notably, the previously determined "trimetallofullerene" (namely, "$Sc_3@C_{3v}$-C_{82}") unambiguously reconfirmed that a Sc_3C_2 cluster is trapped in the $I_h(7)$-C_{80} cage.[17]

Obviously, an opening question is whether a fullerene cage can contain three or more metal atoms without any nonmetal atoms. Earlier, some proposed trimetallofullerenes such as Er_3C_{74},[18] Tb_3C_{80},[19] and Dy_3C_{98}[20] were detected by mass spectrometry (MS). However, there were no further characterizations except a few ambiguous UV−vis−NIR spectroscopies at that time. In 2010, Y_3C_{80} was obtained during the synthesis of nitride clusterfullerenes $Y_3N@C_{2n}$ ($2n$ = 80−88).[21] An exhaustive computational study around Y_3C_{80} indicated that it should be a genuine trimetallofullerene. An analogous structure could be also proposed for Tb_3C_{80}, while $Dy_3C_2@C_{96}$ seems more appropriate for Dy_3C_{98}, predicted in ref 21 at the same time. Recently, Feng et al.[22] provided direct evidence of the existence of $Sm_3@C_{80}$ by means of X-ray single crystal diffraction (XRD). Absolutely, it is a breakthrough because this is the first time to confirm that trimetallofullerene can survive during the arc-discharge process.

As the first predicted trimetallofullerene, it is still ambiguous whether the Er_3C_{74} is a genuine trimetallofullerene $Er_3@C_{74}$ or a trimetal carbide clusterfullerene $Er_3C_2@C_{72}$. It should be pointed out that Er_3C_{74} was recognized as an $Er_3@C_{74}$ structure

Received: June 10, 2015
Published: July 31, 2015

DOI: 10.1021/acs.inorgchem.5b01312
Inorg. Chem. 2015, 54, 8066−8076

Table 1. Relative Energies and Gaps of Er_3C_{74} Isomers

				6-31G(d) for C atoms		6-311G(d) for C atoms	
spiral ID	sym	PA[a]	spin-multiplicity	relative energy (kcal mol^{-1})	gap (eV)	relative energy (kcal mol^{-1})	gap (eV)
C_{74}-14246	D_{3h}	0	nonet	0.0	0.99	0.0	0.98
C_{74}-13771	C_1	2	nonet	6.4	1.03	6.7	1.02
C_{74}-13492	C_3	3	nonet	6.6	1.08	7.0	1.08
C_{74}-13336	C_s	2	nonet	11.0	0.99	11.1	0.99
C_{74}-13295	C_2	2	nonet	12.4	1.15	12.2	1.16
C_{74}-13479	C_1	3	nonet	15.2	1.08	15.6	1.07
C_{74}-13549	C_1	2	nonet	15.4	0.92	15.7	0.92
C_{74}-13408	C_1	2	nonet	18.5	1.27	18.3	1.28
C_{74}-13410	C_1	2	nonet	19.4	0.96	19.7	0.96
C_{72}-10528	C_s	2	11-et	73.8	0.88	75.0	0.87
C_{72}-10482	C_1	3	11-et	78.2	0.73	79.2	0.73
C_{72}-10616	C_s	2	11-et	80.5	0.79	81.0	0.82
C_{72}-10468	C_1	3	11-et	82.8	0.98	83.3	1.01
C_{72}-10518	C_1	3	11-et	92.7	0.90	93.3	0.92

because carbide cluster fullerenes were not discovered at that time.[23] Although the Er_3C_{74} has been characterized by LD-TOF mass spectrum and UV−vis−NIR absorption spectroscopy,[18] the electronic absorption spectrum of the trierbium metallofullerene is featureless, and absorption peaks are very weak. As a result, any further experimental characterization and study are not probable. Hence, a quantum chemical characterization seems to be the best way to determine the structure of the most appropriate Er_3C_{74} isomer and investigate its physical/chemical properties. In this paper, precise studies on a series of Er_3C_{74} isomers including $Er_3@C_{74}$ and $Er_3C_2@C_{72}$ species by means of density functional theory (DFT) combined with statistical thermodynamics calculations have been employed to disclose the most proper structure and interactions among those three metal atoms as well as between a metal atom and the carbon cage.

Particularly, C_{74} EMFs are still less known species due to a low availability. Although several C_{74}-EMFs have been investigated, most of them are monometallofullerenes with the same D_{3h}-C_{74} cage[3] which is the only IPR isomer[24] among all C_{74} cages. Some representative examples of well-studied C_{74}-EMFs include La@C_{74}[25] and its $C_6H_3Cl_2$ derivative[26] as well as a series of $M^{II}@C_{74}$ (M = Ca,[27] Ba,[28] Sr,[29] Eu,[30] Sm,[31−33] and Yb[34,35]). Previously, another two C_{74} cages which are non-IPR species are proposed to encapsulate two scandium atoms.[36] However, the carbide clusterfullerene $Sc_2C_2@C_s(10528)$-C_{72} is the genuine structure of Sc_2C_{74} confirmed by XRD and ^{13}C NMR methods.[37] To the best of our knowledge, the only confirmed C_{74}-EMF containing more than one metal atom is $Sc_2S@C_2(13333)$-C_{74}.[38] That is an ellipsoidal cage with two adjacent pentagon rings locating almost on the opposite poles of the fullerene. It seems that the cage is not appropriate for encapsulating a trierbium cluster.[39] Hence, the study of Er_3C_{74} isomers is not only to disclose the most appropriate cage structure and metal position, but also to provide a comprehensive understanding of the interplay between multimetal atoms and a relatively small fullerene cage.

2. COMPUTATIONAL DETAILS

It has been widely accepted that the concept of endohedral metallofullerenes is described as zwitterions with the metal cation encapsulated in the negatively charged carbon cage. In most cases of erbium-containing EMFs, the oxidation state of an erbium atom is 3+, while it can also adopt the 2+ oxidation state as in $Er_2@C_{82}$ isomers.[3,40] As for $Er_3@C_{74}$ species, the endohedral Er_3 cluster is not mediated by a negatively charged N atom or C_2 group. If the oxidation state of one erbium atom for $Er_3@C_{74}$ were 3+, a huge total number of nine electrons transferring from three erbium atoms to the carbon cage would take place, leading to strong Coulomb repulsion. Consequently, it is reasonable that the formal oxidation state of one erbium atom in $Er_3@C_{74}$ isomers is 2+; those $(Er^{2+})_3$ clusters donate six electrons to C_{74} cages. Meanwhile, the oxidation state of one erbium atom in $Er_3C_2@C_{72}$ species stays its normal 3+, which is similar to that in $Er_2C_2@C_{82}$.[40] The C_2 moiety can accept two electrons formally, so the charge of C_{72} cage is −6. Notably, when dealing with Y_3C_{80} and Dy_3C_{98} systems, the same treatment was performed by Popov et al.[22] The energetics for all those 3099 C_{72}^{6-} and 4603 C_{74}^{6-} anions were first screened at the AM1[41] level, and those results are partially listed in Tables S1 and S2 of the Supporting Information. The number of adjacent pentagons of those C_{72} and C_{74} cages is no more than five. Then, 32 C_{72} and 29 C_{74} cages were chosen as the candidate cages, of which relative energies are all less than 30 kcal mol^{-1}. Those isomers on the hexa-anion state were reoptimized by the hybrid density functional B3LYP[42−44] with 6-31G(d) basis set (see Tables S3 and S4, Supporting Information).

In order to find those energetically favorable Er_3C_{74} isomers, a five-step optimization is applied. The hybrid density functional with unrestricted algorithm UB3LYP was selected from the first to the fourth step. At the first step, 13 C_{74} isomers with the relative energy of hexa-anion less than 30 kcal mol^{-1} and those cages of top-20 C_{72}^{6-} anions were primordially selected to encapsulate a trierbium and trierbium carbide cluster, respectively. Meanwhile, three more C_{72} cages (namely, $C_1(10538)$-C_{72}, $C_s(11080)$-C_{72}, and $C_1(10689)$-C_{72}) were also included. Because a large number of Er_3C_{74} isomers needs to be computed, the smallest basis set STO-3G was used on C atoms, and the Stuttgart/Dresden (SDD) basis set[45] with the ECP28MWB_SEG core potential[46] was applied to erbium atoms. The results are collected in Supporting Information Table S5. It should be pointed out that the erbium-based EMFs lack detailed computational studies because of difficult theoretical treatment of the erbium atoms with 4f electrons. Very recently, a series of *N,N*-dimethylaminodiboranate complexes including erbium atoms was investigated by the same basis set for erbium atoms.[47] Next, according to the results of the first step, some $Er_3@C_{74}$ and $Er_3C_2@C_{72}$ isomers were reoptimized at the UB3LYP/6-31G(d)-SDD~ ECP28MWB_SEG level of theory. The order of their relative energy is shown in Table 1. Then, in order to clarify that the 6-31G(d) basis set is accurate enough for the Er_3C_{74} system, single point and further reoptimization calculations of nine $Er_3@C_{74}$ and five $Er_3C_2@C_{72}$ isomers were performed at UB3LYP/6-311G(d)-SDD~ ECP28MWB_SEG level of theory at the third step, of which configurations were taken from the optimization results of the second step. The result of further reoptimization at B3LYP/6-311G(d)-SDD~ ECP28MWB_SEG level has also been collected in Table 1.

DOI: 10.1021/acs.inorgchem.5b01312
Inorg. Chem. 2015, 54, 8066−8076

Meanwhile, a comparison between the single point calculation and further reoptimization is made in Supporting Information Table S6 and Figure S1. Finally, four lowest-energy $Er_3@C_{74}$ isomers and the $Er_3C_2@C_s(10528)$-C_{72} which possesses the lowest relative energy in trierbium carbide clusterfullerene series were checked by PBE1PEB density functional[48] with 6-311G(d) and Stuttgart RSC 1997 ECP[49] basis sets for C and erbium atoms, respectively. Still, the ECP28MWB_SEG effective core potential is employed for erbium atoms (please see Table S7 in the Supporting Information).

In order to verify whether all stationary points were global minima, a vibrational frequency analysis was performed at the UB3LYP/3-21G*~SDD-ECP28MWB_SEG level of theory. On the basis of frequency analysis, rotational−vibrational partition functions can also be gained, and then relative concentration investigations of the Er_3C_{74} isomers were provided. Notably, it has been confirmed by XRD that the relevance of the thermal and entropic contributions to the stability of fullerene isomers cannot be neglected.[50−52] All of the DFT calculations mentioned above were performed using the Gaussian09 package.[53]

For investigation of the bonding nature of the most promising synthesized Er_3C_{74} isomers, the bonding critical point (BCP) indicator derivative from quantum theory of atoms-in-molecule (QTAIM),[54] Mayer bond order (MBO)[55−57] together with their two-dimensional electron localization function (ELF),[58−60] and Laplacian of electron density maps were examined using the MULTIWFN 3.2.1 program.[61]

3. RESULTS AND DISCUSSION

3.1. Relative Energies and Thermodynamic Stabilities of Er_3C_{74} Series. The relative energy order of the $Er_3C_2@C_{72}$ isomers is drastically different from that of the empty C_{72}^{6-} hexa-anions. The most stable isomer of C_{72}^{6-} among all studied structures is D_2: 10611, and other isomers are less stable by at least 18.0 kcal mol^{-1} (see Supporting Information Table S3). Nevertheless, the $Er_3C_2@D_2(10611)$-C_{72} is 17.8 kcal mol^{-1} less stable than the $Er_3C_2@C_s(10528)$-C_{72} which possesses the lowest energy among all trierbium carbide cluster isomers of the Er_3C_{74} series (see Supporting Information Table S5). Due to the large energy gap between them, the $Er_3C_2@D_2(10611)$-C_{72} is no longer taken into account in following steps. When the 6-31G(d) and 6-311G(d) basis sets are applied to all carbon atoms, the energy of the structure with the C_s: 10528 cage is still the lowest one. $Er_3C_2@C_{72}$ (C_s: 10528) is ~4 and ~6 kcal mol^{-1} more stable than $Er_3C_2@C_{72}$ (C_1: 10482) and $Er_3C_2@C_{72}$ (C_s: 10616), respectively (see Table 1 and Supporting Information Table S6). The correlation between the relative energy order of $Er_3@C_{74}$ and C_{74}^{6-} isomers resembles the situation discussed above for the C_{72} cage (comparing Supporting Information Table S4 and Table 1). As for the hexa-anions of C_{74} species, the ellipsoidal $C_2(13295)$-C_{74} is the most stable empty cage of which potential energy is 5.3 kcal mol^{-1} lower than that of another ellipsoidal $C_2(13333)$-C_{74} cage. The only IPR isomer of C_{74}, D_{3h}: 14246, is 7.1 kcal mol^{-1} less stable in the hexa-anionic state than the isomer $C_2(13295)$-C_{74}. On the other hand, the most stable isomer of $Er_3@C_{74}$ is based on the D_{3h}: 14246 cage. The second and third most stable isomers of $Er_3@C_{74}$, C_1: 13771 and C_3: 13492, are also based on the relatively unstable hexa-anionic cage, of which potential energies are significantly higher by 25.8 and 17.7 kcal mol^{-1}, respectively. Meanwhile, relative energies of $Er_3@C_2(13295)$-C_{74} and $Er_3@C_2(13333)$-C_{74} are about ~13 and ~28 kcal mol^{-1} higher than that of the $Er_3@D_{3h}(14246)$-C_{74}, respectively (see Table 1 and Supporting Information Table S5). The energy difference between $Er_3@C_2(13333)$-C_{74} and $Er_3@D_{3h}(14246)$-C_{74} is so large that we did not consider the $Er_3@C_2(13333)$-C_{74} isomer in the following steps.

It is noteworthy that Popov et al. also found that the stability orders of $M_3N@C_{72}$ and $M_3N@C_{74}$ are drastically different from those of the C_{72}^{6-} and C_{74}^{6-} hexa-anions, respectively. Meanwhile, divergent M_3N clusters (i.e., M = Sc or Y) have significant influences on the stability order of $M_3N@C_{2n}$ isomers ($2n$ = 72 or 74).[39] Consequently, when a relatively large metallic cluster, especially one which transfers six electrons to a carbon cage formally such as Er_3, Er_3C_2, Sc_3N, or Y_3N, is encapsulated in a relatively small C_{72} or C_{74} cage, those energetically favorable isomers in terms of the relative energy of their anionic cages should be carefully confirmed. On the other hand, no charged hollow fullerene isomers that are very energetically unfavorable are found to become favorable when the neutral cage is encapsulated by a metallic cluster. Consequently, it can be guaranteed that the thermodynamic isomers of Er_3C_{74} have been included in the array when those C_{74}^{6-} and C_{72}^{6-} isomers with relative energy less than as high as 30 kcal mol^{-1} are chosen as the pristine candidate to encapsulate an Er_3 or Er_3C_2 cluster.

When the $Er_3@C_{74}$ and $Er_3C_2@C_{72}$ isomers are investigated together, the relative energy of a trierbium carbide cluster isomer is at least 73 kcal mol^{-1} higher than that of the most stable endohedral trierbium isomer. Such high relative energies of those $Er_3C_2@C_{72}$ isomers reveal that the encapsulation of a trierbium carbide cluster in any C_{72} cages is not energetically favorable, compared with that of a trierbium cluster in those specific C_{74} cages.

Further, single point and reoptimization calculations of nine $Er_3@C_{74}$ and five $Er_3C_2@C_{72}$ isomers were performed at UB3LYP/6-311G(d)-SDD~ECP28MWB_SEG level of theory, of which pristine configurations were taken from the optimization results of the second step. As depicted in Supporting Information Table S6 and Figure S1, all differences of those potential energies obtained by single point calculation and reoptimization are very small, and the distribution of them is close (i.e., from 0.22 to 0.31 kcal mol^{-1}). Meanwhile, gaps between the highest occupied molecular orbitals (HOMOs) and the lowest unoccupied molecular orbitals (LUMOs) acquired by single point calculation and reoptimization are almost the same with regard to all referred Er_3C_{74} isomers. Next, those top-four $Er_3@C_{74}$ isomers and the $Er_3C_2@C_s(10528)$-C_{72} were checked by PBE1PBE density functional with the Stuttgart RSC 1997 ECP basis set for erbium atoms (see section VI of Supporting Information). As shown in Supporting Information Table S7, the relative energy order of all Er_3C_{74} species does not have any changes, compared with the order depicted in Table 1. The calculations above prove that the energy order of Er_3C_{74} isomers listed in Table 1 is objective.

Although trierbium carbide cluster fullerenes seem inappropriate due to quite high relative energies, differences of relative energy among those $Er_3@C_{74}$ isomers shown in Table 1 are close. A lot of previous theoretical studies showed that relative stabilities in an isomeric system at high temperatures cannot be simply predicted from the potential energy, as stability interchanges induced by the enthalpy−entropy interplay are possible.[62] This explains why some isomers which may not be the lowest energy one also can be isolated experimentally.[51,52] Consequently, equilibrium statistical thermodynamic calculations based on vibrational analyses are very necessary to confirm the thermodynamic stability of Er_3C_{74} species at high temperature. The calculated relative concentrations of nine

DOI: 10.1021/acs.inorgchem.5b01312
Inorg. Chem. 2015, 54, 8066−8076

$Er_3@C_{74}$ and four $Er_3C_2@C_{72}$ isomers in a wide temperature region have been shown in Figure 1.

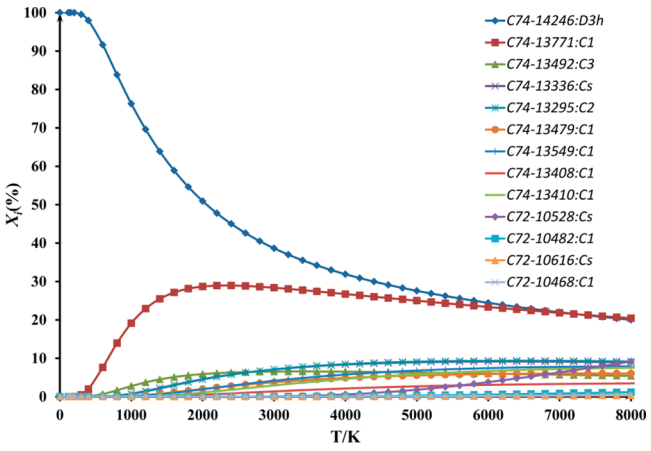

Figure 1. Relative concentrations of Er_3C_{74} isomers.

It is shown that $Er_3@D_{3h}(14246)$-C_{74} prevails at low temperature because of the lowest potential energy, but its concentration decreases significantly with the increase of temperature. At the same time, the concentration of another isomer, $Er_3@C_1(13771)$-C_{74}, increases dramatically when the temperature is over 400 K. At about 2400 K, the relative concentration of $Er_3@C_1(13771)$-C_{74} ascends to its maximum yield of about 29%, compared with a 48% fraction of the $Er_3@D_{3h}(14246)$-C_{74}. After 2400 K, the concentration of $Er_3@C_1(13771)$-C_{74} declines slowly. When the temperature reaches as high as 5000 K, its fraction stays at about 25% with respect to a 27% faction of $Er_3@D_{3h}(14246)$-C_{74}. Overall, the molar faction of $Er_3@D_{3h}(14246)$-C_{74} is overwhelming over the entire temperature range. Other Er_3C_{74} isomers do not display any distinct fraction throughout the whole temperature region. Since the formation of endohedral metallofullerene takes place in the temperature range from 500 to 3000 K,[63] the $Er_3@D_{3h}(14246)$-C_{74} isomer is the most thermodynamically stable isomer and should be experimentally synthesized preferentially. Another trierbium endohedral fullerene $Er_3@C_1(13771)$-C_{74} also possesses relatively high thermodynamic stability. Thus, it is reasonable to conclude that this structure should also be an experimental product. To the best of our knowledge, an endohedral metallofullerene containing the $C_1(13771)$-C_{74} cage has never been reported before.

It is noteworthy that the $C_s(10528)$-C_{72} is important because several C_{72}-based endohedral metallic clusterfullerenes contain this cage such as $Sc_2S@C_{72}$[64] and $Sc_2C_2@C_{72}$.[37] As for the $Er_3C_2@C_s(10528)$-C_{72} here, its formation tendency is still obvious. That is, a considerable concentration of $Er_3C_2@C_s(10528)$-C_{72} could exist if we suppose that it would not pyrolyze at a quite high-temperature region (i.e., over 6500 K). Consequently, it can be inferred that the formation of the trierbium carbide clusterfullerene did not take place due to the fairly high relative energy of $Er_3C_2@C_s(10528)$-C_{72} compared with that of $Er_3@D_{3h}(14246)$-C_{74}. Supposing the relative energy of $Er_3C_2@C_s(10528)$-C_{72} was factitiously reduced to $^1/_3$ of its current value, its concentration at the temperature region of fullerene formation would rise significantly (compare Supporting Information Figure S2 with Figure 1). Due to the low relative energy and suitable enthalpy−entropy interplay, it can be confirmed that the previously reported Er_3C_{74} is a genuine trimetallofullerene, $Er_3@C_{74}$. Both $Er_3@D_{3h}(14246)$-C_{74} and $Er_3@C_1(13771)$-C_{74} can be experimentally synthesized.

3.2. Geometries and Binding Energies of Two Thermodynamically Favorable Er_3C_{74} Isomers. Since $Er_3@C_1(13771)$-C_{74} also has relatively high thermodynamic stability, we will discuss $Er_3@D_{3h}(14246)$-C_{74} and $Er_3@C_1(13771)$-C_{74} together. Those two optimized structures are depicted in Figure 2. Meanwhile, the structures of $Er_3@C_2(13333)$-C_{74} are presented in Figure S3 of Supporting Information for a comparison. The cage of the most thermodynamically stable Er_3C_{74} isomer is the unique IPR one in the C_{74} series, which has D_{3h} symmetry, while the encapsulation of a trierbium cluster causes the symmetry reduction to C_s. Each erbium atom resides under a six-membered ring [see Figure 2 (top)]. Distances between the centers of two six-membered rings connected with erbium atoms are about 6.48, 6.90, and 6.88 Å, forming almost an equilateral triangle. Moreover, all three metal-to-ring-centroid distances are approximately 1.95 Å. Consequently, three erbium atoms also form a proximate equilateral triangle with Er−Er distances ranging from 3.42 to 3.51 Å, which are comparable those in $Sc_3N@I_h$-C_{80} (d_{Sc-Sc} = 3.490−3.510 Å)[65] and $Gd_3N@I_h$-C_{80} (d_{Gd-Gd} = 3.409−3.449 Å),[66] but longer than those in $Sm_3@I_h$-C_{80} (d_{Sm-Sm} = 3.173−3.313 Å).[22] It is indicated that the +3 oxidation state of erbium atoms is improper for the present $Er_3@D_{3h}(14246)$-C_{74} due to a smaller ionic radius of Er^{3+} compared with that of Gd^{3+}. In addition, all three metal-to-ring-centroid distances in $Er_3@D_{3h}(14246)$-C_{74} (1.95 Å) are shorter than those in $Sm_3@I_h$-C_{80} (~2.1 Å),[22] proving a larger nanoscale fullerene compression[67] of a trierbium cluster in the relatively small $D_{3h}(14246)$-C_{74} cage than that of a trisamarium one in the I_h-C_{80} cage.

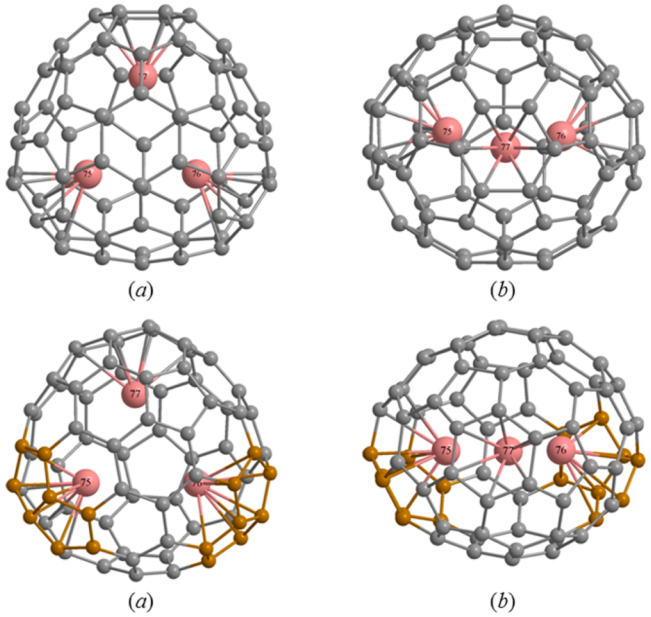

Figure 2. (a) Side and (b) top views of optimized $Er_3@D_{3h}(14246)$-C_{74} (top) and $Er_3@C_1(13771)$-C_{74} (bottom) structures. Erbium atoms and pentalene units are colored pink and gray, respectively, for emphasis.

The $C_1(13771)$-C_{74} and $C_2(13333)$-C_{74} cages violate the well-known isolated pentagon rule (IPR)[24] with two pentalene units [see Table 2 (bottom) and Supporting Information

DOI: 10.1021/acs.inorgchem.5b01312
Inorg. Chem. 2015, 54, 8066−8076

Table 2. BCP Parameters and Values of Mayer Bond Order (MBO) for Er−Cage Interactions

bond	D^a (Å)	ρ_{BCP} (au)	$\nabla^2\rho_{BCP}$ (au)	H_{BCP} (au)	$\lvert V_{BCP}\rvert/G_{BCP}$ (au)	ε	MBO
			$Er_3@D_{3h}(14246)$-C_{74}				
Er75−C8	2.420	0.058	0.18	−0.0099	1.18	2.77	0.25
Er75−C9	2.399	0.060	0.19	−0.011	1.19	2.13	0.25
Er75−C10	2.403	0.060	0.19	−0.011	1.19	3.07	0.24
Er75−CS7	2.439	0.056	0.18	−0.0087	1.16	9.54	0.23
Er75−CS8	2.426	0.056	0.18	−0.0096	1.17	2.65	0.24
Er75−CS9	2.421	0.058	0.18	−0.010	1.18	2.71	0.24
Er76−C67	2.396	0.060	0.19	−0.011	1.19	1.52	0.25
Er76−C20	2.393	0.060	0.19	−0.011	1.19	1.70	0.25
Er77−C42	2.364	0.065	0.20	−0.014	1.21	3.33	0.26
Er77−C43	2.367	0.065	0.20	−0.013	1.21	3.89	0.26
			$Er_3@C_1(13771)$-C_{74}				
Er75−C9	2.397	0.059	0.20	−0.010	1.18	1.74	0.23
Er75−C10	2.399	0.061	0.19	−0.012	1.19	1.03	0.23
Er75−CS9	2.415	0.058	0.19	−0.010	1.18	3.12	0.24
Er76−C64	2.437	0.056	0.19	−0.0089	1.16	1.72	0.23
Er76−C65	2.417	0.059	0.19	−0.011	1.19	0.11	0.22
Er76−C66	2.450	0.053	0.18	−0.0081	1.15	7.11	0.22
Er77−CS0	2.335	0.067	0.21	−0.015	1.21	0.75	0.27

$^a D$ = bond length.

Figure S3]. When they encapsulate trierbium clusters, each pentagon adjacent unit is bonded with an erbium atom, while it is uncommon that all metal atoms are not located closely to [5, 5]-bonds of fused pentagons.[37,64,68] The third erbium atom is located close to a six-membered ring. In $Er_3@C_1(13771)$-C_{74}, the range of Er−Er distances is from 3.39 to 3.68 Å, which is somewhat wider than that in $Er_3@D_{3h}(14246)$-C_{74}. On the other hand, as shown in Supporting Information Table S8, erbium−erbium distances in either $Er_3@D_{3h}(14246)$-C_{74} or $Er_3@C_1(13771)$-C_{74} are significantly shorter than those of a bare Er_3 cluster. This is an obvious result because a large metallic cluster is trapped in a relatively small C_{74} cage, leading to nanoscale fullerene compression. The decrease of Er−Er distances causes the increase of Er−Er repulsion, so the bare Er_3 cluster with the same configuration as that captured in the $D_{3h}(14246)$-C_{74} or $C_1(13771)$-C_{74} cage possesses much higher potential energy and positive binding energy, compared with the optimized trierbium cluster. Accordingly, it can be inferred that the former cannot be synthesized and isolated without the protection of a fullerene cage.

As for the $Er_3@C_2(13333)$-C_{74}, due to a large separation of two pentalenes (i.e., ∼8.98 Å), the distance between those two Er atoms which are close to pentagon adjacent units (Er75−Er76, see Supporting Information Figure S3) is as large as 4.4 Å. At the same time, distances between Er75 and Er77 as well as Er76 and Er77 are shortened to 3.1 and 3.2 Å, respectively, causing somewhat large repulsions. Consequently, $D_{3h}(14246)$-C_{74} becomes the best cage for the trierbium cluster not only because the relative energy of its hexa-anion is relatively low, but also because it possesses a high symmetry to reduce repulsions among erbium atoms as far as possible. Meanwhile, although the relative energy of $C_1(13771)$-C_{74}^{6-} is relatively high (ΔE = 25.8 kcal mol^{-1}, see Supporting Information Table S4), the $Er_3@C_1(13771)$-C_{74} can survive because it has the appropriate location of the pentalene motifs to optimize the interaction with erbium atoms.

The fact that the thermodynamically stable Er_3C_{74} is two $Er_3@C_{74}$ isomers rather than an $Er_3C_2@C_{72}$ one also can be explained from the deformation of their carbon cages after encapsulation. As shown from Supporting Information Figures S4 to S6, the encapsulation of a trierbium or trierbium carbide cluster expands all carbon cages. Compared with $D_{3h}(14246)$-C_{74} and $C_1(13771)$-C_{74} cages, the deformation of $C_s(10528)$-C_{72} cage is more obvious because a bigger Er_3C_2 cluster is encapsulated in the smaller C_{72} cage compared with a Er_3 cluster and those C_{74} cages. The deformation causes destabilization of those carbon cages. We have calculated the deformation energy that is defined as the difference between the single point energy of a cage strained by an Er_3/Er_3C_2 cluster and the optimized energy of that cage with restrictions at the same level of theory as well as HOMO−LUMO gap of those three hexa-anionic cages at free and strained status. Generally speaking, the expansion of all carbon cages leads to an increase of their potential energies, comparing the single point energy of one strained C_{74} or C_{72} hexa-anion with the energy obtained by the optimization of the corresponding hexa-anion with no restrictions, causing positive deformation energies of those fullerene cages. At the same time, HOMO−LUMO gaps of all strained hexa-anions significantly decrease, compared with those of free ones, giving rise to a reduction of their kinetic stabilities. As presented in Supporting Information Table S9, the $C_s(10528)$-C_{72} hexa-anion possesses the largest deformation energy and the narrowest HOMO−LUMO gap among those considered isomers due to its serious deformation. Although the deformation of the $D_{3h}(14246)$-C_{74} cage is somewhat greater than that of $C_1(13771)$-C_{74} after encapsulation, the $Er_3@D_{3h}(14246)$-C_{74} still possesses the lowest potential energy as a consequence of the noticeably lower potential energy of the free $D_{3h}(14246)$-C_{74}^{6-} anion, compared with that of the free $C_1(13771)$-C_{74}^{6-} one.

To further clarify the thermodynamic stabilities of $Er_3@D_{3h}(14246)$-C_{74} and $Er_3@C_1(13771)$-C_{74} molecules, their binding energies including basis set superposition error (BSSE) correction have been calculated at UB3LYP/6-31G(d)-SDD∼ECP28MWB_SEG level of theory. As tabulated in Table S10 of Supporting Information, both $Er_3@C_{74}$ structures have negative enough binding energies to keep endohedral configurations. Interestingly, the absolute value of

DOI: 10.1021/acs.inorgchem.5b01312
Inorg. Chem. 2015, 54, 8066−8076

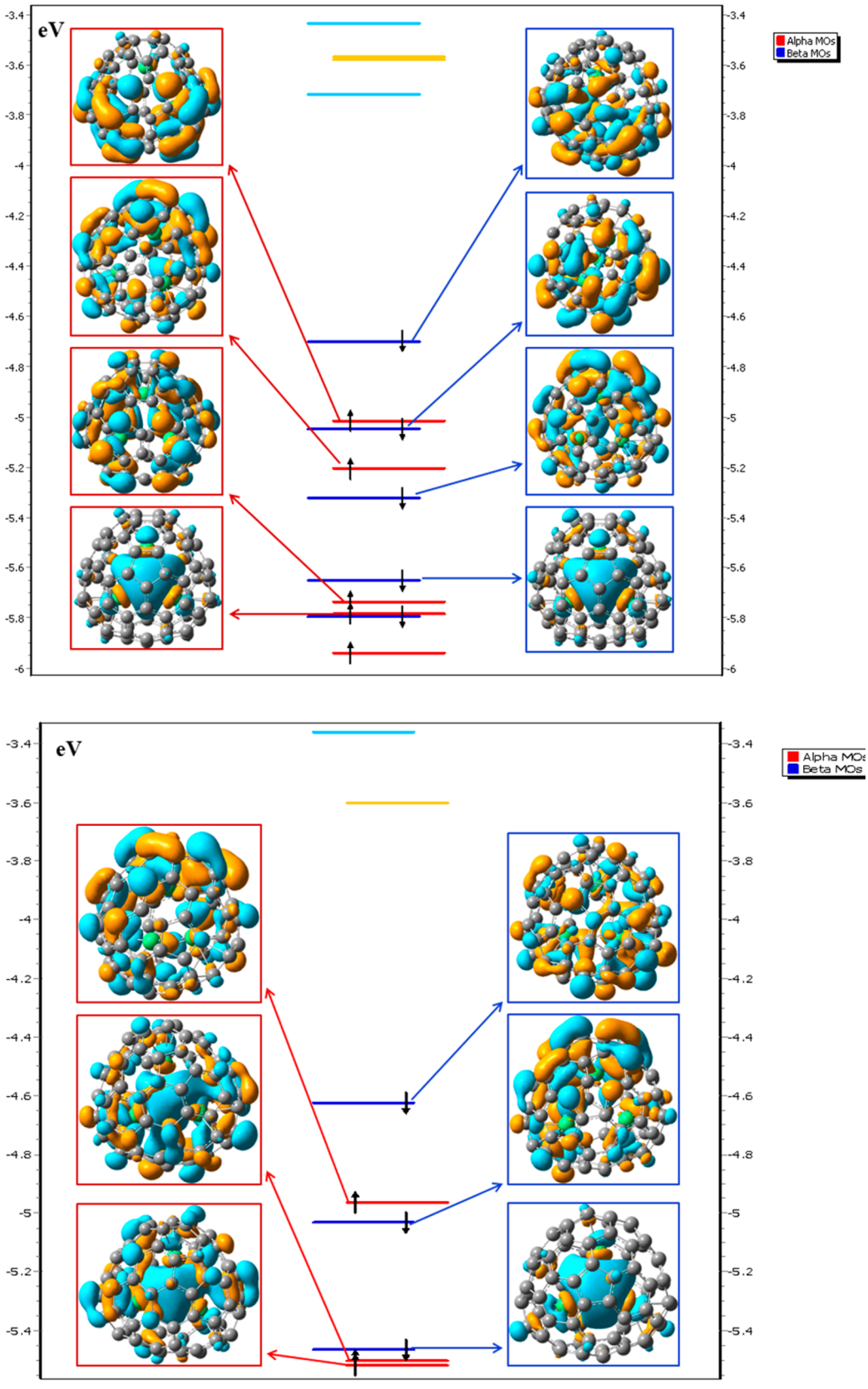

Figure 3. Main occupied frontier orbital diagrams of $Er_3@D_{3h}(14246)$-C_{74} (top) and $Er_3@C_1(13771)$-C_{74} (bottom).

binding energy for $Er_3@C_1(13771)$-C_{74} is 31 kcal mol^{-1} larger than that for $Er_3@D_{3h}(14246)$-C_{74} although the former isomer possesses lower relative energy. This indicates that the interactions between the $C_1(13771)$-C_{74} cage and trierbium cluster are stronger than that between the $D_{3h}(14246)$-C_{74} one and the same metallic moiety. The more negative binding energy for $Er_3@C_1(13771)$-C_{74} plays an important role in compensating for the lesser stability of the low-symmetry cage.

DOI: 10.1021/acs.inorgchem.5b01312
Inorg. Chem. 2015, 54, 8066−8076

Consequently, after the capture of a trierbium cluster, the energy gap between those two isomers is only 6.7 kcal mol^{-1}, while it is as large as 25.8 kcal mol^{-1} between two hexa-C_{74} anions.

3.3. Electronic Structures and Bonding Natures. As mentioned above, the oxidation state of erbium atoms encapsulated in C_{74} cages should be +2 rather than its common +3. Consequently, it can be expected that special electronic structures and bonding patterns exist in thermodynamically stable Er_3C_{74} isomers, namely, $Er_3@D_{3h}(14246)$-C_{74} and $Er_3@C_1(13771)$-C_{74}. As shown at the top of Figure 3, most occupied frontier orbitals of $Er_3@D_{3h}(14246)$-C_{74} are mainly located on the fullerene cage with relatively substantial orbital overlaps between metal atomic orbitals and those belonging to the $D_{3h}(14246)$-C_{74} cage, revealing that covalent interactions between erbium atoms and the cage cannot be ignored. This is quite different from the situation of $Sm@D_{3h}$-C_{74} in which metal−cage interactions are weak, as studied by Feng et al.[33] Consequently, it can be inferred that the bonding situation of a endohedral metallofullerene should be determined by the carbon cage and the encapsulated moiety together. At the same time, there are two single occupied orbitals which are totally symmetric, with predominant contributions from s atomic orbitals of three erbium atoms. This kind of orbital is similar to "interstitial" orbitals known for metal clusters, previously described by Goddard et al.[69] As for the $Er_3@C_1(13771)$-C_{74} isomer, prominent covalent interactions between erbium atoms and the cage cannot also exist, as concluded from those occupied frontier molecular orbitals hybridized by metal atomic orbitals and cage orbitals (see bottom of Figure 3). In addition, there are two almost degenerate α- and a β-single occupied molecular orbitals possessing "interstitial" characteristics. The trivial difference of electronic structures between $Er_3@D_{3h}(14246)$-C_{74} and $Er_3@C_1(13771)$-C_{74} may ascribe the divergent orbital distributions of their fullerene cage. Besides, we also have found several other orbitals with "interstitial" characteristics among low-energy unoccupied orbitals, depicted in Figure S7 in the Supporting Information. Interestingly, all of them belong to α-orbitals.

Covalent interactions between erbium atoms and carbon cage in both $Er_3@D_{3h}(14246)$-C_{74} and $Er_3@C_1(13771)$-C_{74} have been further studied utilizing the quantum theory of atoms-in-molecule (QTAIM)[54] and Mayer bond order (MBO)[55−57] approaches. Molecular graphs of those two isomers obtained by the MULTIWFN 3.2.1 program[61] are shown in Figure S8 of Supporting Information. For $Er_3@D_{3h}(14246)$-C_{74}, each erbium atom resides upon a six-membered ring, while only the Er75 exhibits six bond paths to the carbon atoms of its hexagon. Er76 and Er77 bond to a 6−6 bond (C20−C67) and a 5−6 bond (C42−C43), respectively. In $Er_3@C_1(13771)$-C_{74}, whose cage is a non-IPR one with two pentagon adjacent units, each of the Er75 and Er76 atoms is near to a pentalene fragment with a three bond path. Meanwhile, the Er77 atom is located near a six-membered ring, whereas only one bond path exists between this erbium atom and one carbon atom (i.e., C50) of the hexagon. For a clearer illustration in Figure 4, we omit all bonding critical points (BCPs), and those carbon atoms bonding with erbium ones in the $Er_3@D_{3h}(14246)$-C_{74} or $Er_3@C_1(13771)$-C_{74} cage are light green, while other carbon atoms are represented by gray stick model.

Table 2 shows a series of QTAIM parameters for Er_3−cage interactions in $Er_3@D_{3h}(14246)$-C_{74} and $Er_3@C_1(13771)$-C_{74}.

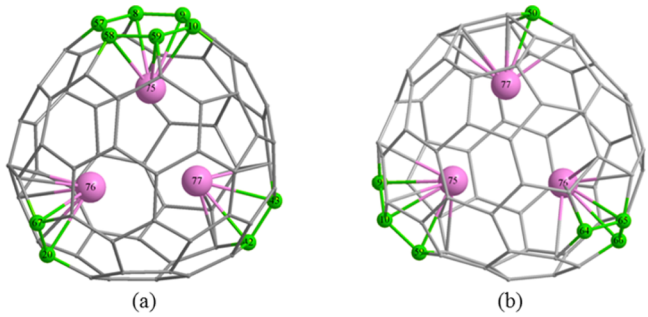

Figure 4. Bonding between encapsulated erbium atoms and carbon atoms in the (a) $Er_3@D_{3h}(14246)$-C_{74} or $Er_3@C_1(13771)$-C_{74} (b) cage. Erbium atoms are pink, and if a bonding critical point exists between an erbium and a carbon atom, the carbon atom is highlighted in light green, based on Supporting Information Figure S8.

Although the number of bond paths between one erbium atom and the carbon cage encapsulating it is different, namely, from one to six, similar strengths of metal−cage interactions can be found clearly in those two trierbium endohedral fullerenes. All values of the electron density (ρ_{BCP}) and its Laplacian ($\nabla^2\rho_{BCP}$) at all BCPs between an erbium atom and a carbon atom in $D_{3h}(14246)$-C_{74} or $C_1(13771)$-C_{74} cage are small and positive with very narrow ranges (0.056−0.067 au for ρ_{BCP}, and 0.18−0.21 for $\nabla^2\rho_{BCP}$), respectively. Popov and Dunsch[4] have pointed out that it is normal for transition metals because of the diffuse character of their electron distributions. Covalent interactions between erbium and carbon atoms can be confirmed by negative values of energy density (H_{BCP}) which range from −0.0081 to −0.015, and relatively large ratios of absolute value of potential energy density to kinetic energy density ($|V_{BCP}|/G_{BCP}$), all of which are large than 1. At the same time, values of bond ellipticity (ε) at different BCPs can vary in a wide range (i.e., from 0.75 to 9.54). Larger values are the characteristic of increasing delocalization of the bond.[70] It is ca. 0.23 in benzene and 0.45 in ethylene, suggesting that all Er−C bonds possess obvious π character. Significantly, most values of ε are larger than 2, and one of them (Er75−C57 in $Er_3@D_{3h}(14246)$-C_{74}) is even as large as 9.54, indicating the dominant delocalization nature of metal−cage interactions which can hardly exist in normal small molecular π system. Additionally, a such high value of ε has also been discovered by Chen et al.[71] when they studied the $Sc_3CN@C_{2n}$ ($2n$ = 68, 78, and 80) series.

Also shown in Table 2, values of Mayer bond order for Er−cage interactions in $Er_3@D_{3h}(14246)$-C_{74} and $Er_3@C_1(13771)$-C_{74} range from 0.22 to 0.27, which are relatively larger values compared with those of the previously studied $Gd_2C_2@C_{92}$ (0.16−0.21, and generally stay around 0.18)[72] and $Sc_2S@C_{68}$ (in the range 0.17−0.21)[73] systems. As a result, covalent interactions in the thermodynamically stable $Er_3@C_{74}$ isomers are somewhat more conspicuous than other endohedral metallofullerenes studied in the past, and accordingly, this may be another reason why the relative energy order of $Er_3@C_{74}$ isomers is quite different from that of the hexa-anionic C_{74} vacant cage. The total number of the electron pairs shared between each erbium atom and the cage varies from approximately 2.9 to 3.0, which is even remarkably larger than that between each Y atom and C_{80} cage in the $Y_3@I_h$-C_{80} isomer which is the first reported trimetallofullerene.[21]

According to Mulliken charge distributions of $Er_3@D_{3h}(14246)$-C_{74} and $Er_3@C_1(13771)$-C_{74} (see Figure S9 of

DOI: 10.1021/acs.inorgchem.5b01312
Inorg. Chem. 2015, 54, 8066−8076

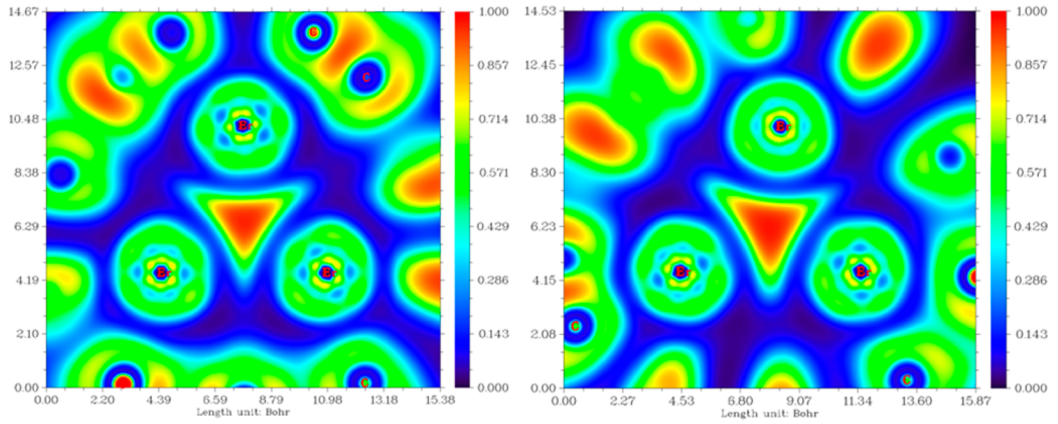

Figure 5. Two-dimensional ELF maps of $Er_3@D_{3h}(14246)$-C_{74} (left) and $Er_3@C_1(13771)$-C_{74} (right) in the plane determined by three erbium atoms.

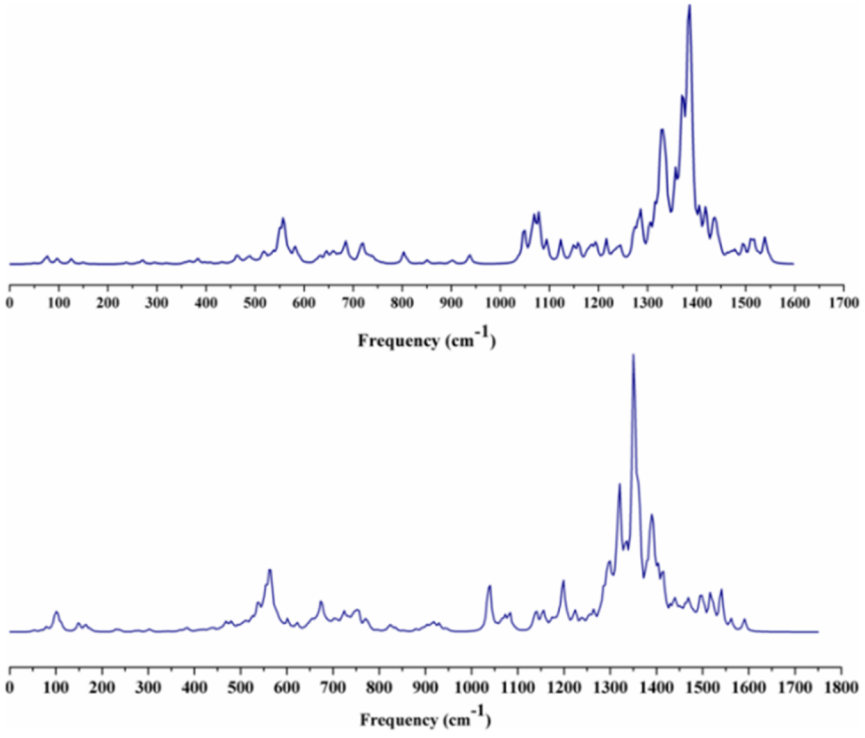

Figure 6. IR spectra of $Er_3@D_{3h}(14246)$-C_{74} (top) and $Er_3@C_1(13771)$-C_{74} (bottom).

Supporting Information), each erbium atom is a center of positive charge. How to overcome the huge repulsion among three metal atoms is an interesting issue to study. As shown in Supporting Information Figure S8, no bond paths or bonding critical points between two erbium atoms can be found. In other words, we cannot find direct evidence for any Er−Er two-center bonds. Further, we plotted two-dimensional electron localization function (ELF)[58−60] and Laplacian of electron density maps of $Er_3@D_{3h}(14246)$-C_{74} and $Er_3@C_1(13771)$-C_{74} in the plane determined by three erbium atoms, which are illustrated in Figure 5 and Supporting Information Figure S10, respectively. A two-dimensional ELF map of the optimized bare Er_3 cluster was also plotted, illustrated in Supporting Information Figure S11. In a comparison of Supporting Information Figure S11 and Figure 5, the ELF map of the optimized bare Er_3 cluster is quite different from that among three erbium atoms inside the $D_{3h}(14246)$-C_{74} and $C_1(13771)$-C_{74} cages. As for the optimized bare Er_3 cluster, three maxima of ELF appear between pairwise erbium atoms, forming three Er−Er two-center bonds. Instead, there is a triangular region surrounded by three erbium atoms in each trierbium endohedral fullerene, in which the value approaches the maximum value of ELF, indicating that electrons are greatly localized among three erbium atoms, forming a three-center covalent bond. This is very consistent with the fact that "interstitial" orbitals exist among three erbium atoms mentioned above. Accordingly, the strong electrostatic repulsion caused by those positively charged erbium atoms can be weakened efficiently. A similar result can also be summarized from the two-dimensional Laplacian of electron density maps of $Er_3@D_{3h}(14246)$-C_{74} and $Er_3@C_1(13771)$-C_{74}. Among three erbium atoms in both maps shown in Supporting Information Figure S10, there is an obvious area where the value of Laplacian of electron density is smaller than zero

DOI: 10.1021/acs.inorgchem.5b01312
Inorg. Chem. 2015, 54, 8066−8076

within two bonding critical points. This is additional evidence for the cohesion of electrons among three erbium atoms.

Interestingly, it seems that different trimetallofullerenes already discussed have different bonding natures. According to Popov et al.'s exhaustive calculations,[21] the single occupied molecular orbital (SOMO) of $Y_3@I_h$-C_{80} is an "interstitial" orbital among three yttrium atoms. Meanwhile, they obtained valid evidence to confirm that a non-nuclear attractor (NNA),[74] which means a maximum of electron density, exists in this zone. In the present $Er_3@C_{74}$ isomers, obvious covalent interactions among three erbium atoms can be concluded, while no NNA can be found. As for the $Sm_3@I_h$-C_{80},[22] the "interstitial" molecular orbital is the LUMO without any electrons. In this case, the region among three samarium atoms cannot be the maximum value of the electron density, its Laplacian, and ELF. Accordingly, it can be inferred that no non-nuclear attractors and covalent interactions exist among three samarium atoms. Consequently, the bonding nature of divergent pure endohedral multimetallofullerenes should be analyzed case-by-case.

3.4. Infrared (IR) Spectra. Since IR spectra of endohedral metallofullerenes are very sensitive to their molecular structures, they help to distinguish structures of different isomers with the same molecular formula.[75,76] Therefore, IR spectra of $Er_3@D_{3h}(14246)$-C_{74} and $Er_3@C_1(13771)$-C_{74} have been simulated in terms of harmonic vibrational analysis as shown in Figure 6, which may be useful for further experimental characterization.

The spectrum of either $Er_3@D_{3h}(14246)$-C_{74} or $Er_3@C_1(13771)$-C_{74} can be mainly divided into four regions. The lowest region from 0 to 170 cm^{-1} is very weak, which is attributed to the stretching and rocking vibration of three encapsulated erbium atoms. The reason why this kind of vibration presents quite low frequencies can be rationalized by the large mass of encapsulated metal atoms.[77] Other three regions all correspond to different vibrations of those two fullerene cages. The 200−760 cm^{-1} region for $Er_3@D_{3h}(14246)$-C_{74} and 200−780 cm^{-1} region for $Er_3@C_1(13771)$-C_{74} correspond to cage breathing mode. In this vibrational mode, their carbon cages expand and shrink alternately. The 800−950 cm^{-1} range of both $Er_3@D_{3h}(14246)$-C_{74} and $Er_3@C_1(13771)$-C_{74} corresponds to rocking vibrations of their cages, and stretching vibrations of C−C bonds range from 1000 to 1600 cm^{-1} which is the last region of the IR spectra.

Fortunately, the IR spectra of $Er_3@D_{3h}(14246)$-C_{74} and $Er_3@C_1(13771)$-C_{74} from 1000 to 1600 cm^{-1} have some differences which are useful for distinguishing those two thermodynamic Er_3C_{74} isomers. The strongest absorption peak of $Er_3@D_{3h}(14246)$-C_{74} is located at 1387 cm^{-1} with an obvious shoulder peak at about 1360 cm^{-1}, while a peak with an analogous absorption intensity but no shoulder peaks appears with a bit of a blue shift at 1350 cm^{-1}. There are two peaks located on either side of the most intense peak in the IR spectrum of $Er_3@C_1(13771)$-C_{74} at 1300 and 1400 cm^{-1}, respectively, while only one peak can be seen to the left of the strongest peak of $Er_3@D_{3h}(14246)$-C_{74} at approximately 1300 cm^{-1}. At the same time, a multiple peak ranging from 1050 to 1100 cm^{-1} can be found followed by a series of weak peaks in the range 1100−1200 cm^{-1}, while there are no multiple peaks in the same region of the IR spectrum of $Er_3@C_1(13771)$-C_{74}. By the way, because there are no C_2 moieties encapsulated in $D_{3h}(14246)$-C_{74} and $C_1(13771)$-C_{74} cages, no vibrational modes with wavenumber larger than 1800 cm^{-1} are found, which corresponds to C−C stretching of the internal C_2 moieties.[76]

4. CONCLUSIONS

A density functional theory combined with a statistical mechanics study has been performed on a series of Er_3C_{74} including $Er_3@C_{74}$ and $Er_3C_2@C_{72}$. Our results uncover that there are two stable isomers, each of which is a genuine trierbium fullerene without any nonmetal atoms in the cage. $Er_3@D_{3h}(14246)$-C_{74} possesses the lowest potential energy with the best thermodynamic stability, and this cage is the unique C_{74} isomer obeying the isolated pentagon rule. $Er_3@C_1(13771)$-C_{74} also has considerable abundance at the temperature region of endohedral metallofullerene formation, and this cage is violating the isolated pentagon rule with two adjacent pentagons. To the best of our knowledge, this is the first time to report an endohedral metallofullerene containing the $C_1(13771)$-C_{74} cage. No $Er_3C_2@C_{72}$ isomers can survive due to their high potential energies. Significantly, the fact that the relative energy order of $Er_3@C_{74}$ is quite different from that of C_{74}^{6-} anions reveals that the traditional ionic interaction model is not appropriate for the present $Er_3@C_{74}$ system, and a proper geometry of one cage seems important to the stabilization of an $Er_3@C_{74}$ isomer. Obvious covalent interactions can be identified from substantial overlaps between metallic orbitals and cage orbitals as well as indicators of bonding critical points and Mayer bond order between erbium atoms and the carbon cage. At the same time, there are no bonding critical points between any two metal atoms, while two-dimensional maps of electron localization function (ELF) and Laplacian of electron density of $Er_3@D_{3h}(14246)$-C_{74} and $Er_3@C_1(13771)$-C_{74} indicate obvious covalent interactions among three erbium atoms. This is very consistent with the fact that "interstitial" orbitals exist among three erbium atoms. The strong electrostatic repulsion caused by those positively charged erbium atoms can be weakened efficiently in this way. It should also be pointed out that different trimetallofullerenes already discussed have different bonding natures, and they should be analyzed case-by-case. IR spectra of $Er_3@D_{3h}(14246)$-C_{74} and $Er_3@C_1(13771)$-C_{74} have been simulated, both of which can be divided into four regions according to different vibrational modes. The IR spectra differences of those two isomers with the wavenumber ranging from 1000 to 1600 cm^{-1} provide a helpful method to distinguish those two Er_3C_{74} isomers.

■ ASSOCIATED CONTENT

Supporting Information

Relative energies of selected C_{72}^{6-} and C_{74}^{6-} anions at AM1 and B3LYP/6-31G(d) levels of theory; relative energies of all selected Er_3C_{74} isomers optimized from the first to the fourth step; relative concentrations of Er_3C_{74} isomers after reduction of the relative energy of $Er_3C_2@C_s(10528)$-C_{72} to $^1/_3$ of its true value; optimized structures of $Er_3@C_2(13333)$-C_{74} and $Er_3C_2@C_s(10528)$-C_{72}; cage deformation of three representative isomers of Er_3C_{74} after encapsulation; several unoccupied molecular orbitals, molecular graphs, Mulliken charge distributions, and Cartesian coordinates of $Er_3@D_{3h}(14246)$-C_{74} and $Er_3@C_1(13771)$-C_{74}. The Supporting Information is available free of charge on the ACS Publications website at DOI: 10.1021/acs.inorgchem.5b01312.

DOI: 10.1021/acs.inorgchem.5b01312
Inorg. Chem. 2015, 54, 8066−8076

AUTHOR INFORMATION

Corresponding Author

*E-mail: xzhao@mail.xjtu.edu.cn. Fax: +86 29 8266 8559. Phone: +86 29 8266 5671.

Notes

The authors declare no competing financial interest.

ACKNOWLEDGMENTS

This work has been financially supported by the National Natural Science Foundation of China (No. 21171138), the National Key Basic Research Program of China (No. 2011CB209404, 2012CB720904), the Specialized Research Fund for the Doctoral Program of Higher Education of China (SRFDP No. 20130201110033), and the 56th Postdoctoral Fund in China (No. 2014M560758).

REFERENCES

(1) Kroto, H. W.; Heath, J. R.; O'Brien, S. C.; Curl, R. F.; Smalley, R. E. *Nature* **1985**, *318*, 162.
(2) Heath, J. R.; O'Brien, S. C.; Zhang, Q.; Liu, Y.; Curl, R. F.; Kroto, H. W.; Tittel, F. K.; Smalley, R. E. *J. Am. Chem. Soc.* **1985**, *107*, 7779.
(3) Popov, A. A.; Yang, S.; Dunsch, L. *Chem. Rev.* **2013**, *113*, 5989.
(4) Popov, A. A.; Dunsch, L. *Chem. - Eur. J.* **2009**, *15*, 9707.
(5) Feng, M.; Twamley, J. *Phys. Rev. A: At., Mol., Opt. Phys.* **2004**, *70*, 030303.
(6) Feng, M.; Twamley, J. *Phys. Rev. A: At., Mol., Opt. Phys.* **2004**, *70*, 032318.
(7) Khlobystov, A. N.; Britz, D. A.; Briggs, G. A. D. *Acc. Chem. Res.* **2005**, *38*, 901.
(8) Ross, R. B.; Cardona, C. M.; Guldi, D. M.; Sankaranarayanan, S. G.; Reese, M. O.; Kopidakis, N.; Peet, J.; Walker, B.; Bazan, G. C.; Van Keuren, E.; Holloway, B. C.; Drees, M. *Nat. Mater.* **2009**, *8*, 208.
(9) Pinzon, J. R.; Plonska-Brzezinska, M. E.; Cardona, C. M.; Athans, A. J.; Gayathri, S. S.; Guldi, D. M.; Herranz, M. A.; Martin, N.; Torres, T.; Echegoyen, L. *Angew. Chem., Int. Ed.* **2008**, *47*, 4173.
(10) Dang, J.-S.; Wang, W.-W.; Zhao, X.; Nagase, S. *Org. Lett.* **2014**, *16*, 170.
(11) Sitharaman, B.; Wilson, L. J. *J. Biomed. Nanotechnol.* **2007**, *3*, 342.
(12) Zhang, J.; Liu, K. M.; Xing, G. M.; Ren, T. X.; Wang, S. K. *J. Radioanal. Nucl. Chem.* **2007**, *272*, 605.
(13) Liu, Y.; Jiao, F.; Qiu, Y.; Li, W.; Lao, F.; Zhou, G.; Sun, B.; Xing, G.; Dong, J.; Zhao, Y.; Chai, Z.; Chen, C. *Biomaterials* **2009**, *30*, 3934.
(14) Stevenson, S.; Mackey, M. A.; Stuart, M. A.; Phillips, J. P.; Easterling, M. L.; Chancellor, C. J.; Olmstead, M. M.; Balch, A. L. *J. Am. Chem. Soc.* **2008**, *130*, 11844.
(15) Mercado, B. Q.; Olmstead, M. M.; Beavers, C. M.; Easterling, M. L.; Stevenson, S.; Mackey, M. A.; Coumbe, C. E.; Phillips, J. D.; Phillips, J. P.; Poblet, J. M.; Balch, A. L. *Chem. Commun.* **2010**, *46*, 279.
(16) Wang, T.-S.; Chen, N.; Xiang, J.-F.; Li, B.; Wu, J.-Y.; Xu, W.; Jiang, L.; Tan, K.; Shu, C.-Y.; Lu, X.; Wang, C.-R. *J. Am. Chem. Soc.* **2009**, *131*, 16646.
(17) Iiduka, Y.; Wakahara, T.; Nakahodo, T.; Tsuchiya, T.; Sakuraba, A.; Maeda, Y.; Akasaka, T.; Yoza, K.; Horn, E.; Kato, T.; Liu, M. T. H.; Mizorogi, N.; Kobayashi, K.; Nagase, S. *J. Am. Chem. Soc.* **2005**, *127*, 12500.
(18) Tagmatarchis, N.; Aslanis, E.; Prassides, K.; Shinohara, H. *Chem. Mater.* **2001**, *13*, 2374.
(19) Lian, Y. F.; Shi, Z. J.; Zhou, X. H.; Gu, Z. N. *Chem. Mater.* **2004**, *16*, 1704.
(20) Yang, S. F.; Dunsch, L. *Angew. Chem., Int. Ed.* **2006**, *45*, 1299.
(21) Popov, A. A.; Zhang, L.; Dunsch, L. *ACS Nano* **2010**, *4*, 795.
(22) Xu, W.; Feng, L.; Calcaresi, M.; Liu, J.; Liu, Y.; Niu, B.; Shi, Z.; Lian, Y.; Zerbetto, F. *J. Am. Chem. Soc.* **2013**, *135*, 4187.
(23) Wang, C.-R.; Kai, T.; Tomiyama, T.; Yoshida, T.; Kobayashi, Y.; Nishibori, E.; Takata, M.; Sakata, M.; Shinohara, H. *Angew. Chem., Int. Ed.* **2001**, *40*, 397.
(24) Fowler, P. W.; Manolopoulos, D. E. *An Atlas of Fullerenes*; Clarendon Press: Oxford, U.K., 1995.
(25) Diener, M. D.; Alford, J. M. *Nature* **1998**, *393*, 668.
(26) Nikawa, H.; Kikuchi, T.; Wakahara, T.; Nakahodo, T.; Tsuchiya, T.; Rahman, G. M. A.; Akasaka, T.; Maeda, Y.; Yoza, K.; Horn, E.; Yamamoto, K.; Mizorogi, N.; Nagase, S. *J. Am. Chem. Soc.* **2005**, *127*, 9684.
(27) Kodama, T.; Fujii, R.; Miyake, Y.; Suzuki, S.; Nishikawa, H.; Ikemoto, I.; Kikuchi, K.; Achiba, Y. *Chem. Phys. Lett.* **2004**, *399*, 94.
(28) Reich, A.; Panthöfer, M.; Modrow, H.; Wedig, U.; Jansen, M. *J. Am. Chem. Soc.* **2004**, *126*, 14428.
(29) Haufe, O.; Hecht, M.; Grupp, A.; Mehring, M.; Jansen, M. *Z. Anorg. Allg. Chem.* **2005**, *631*, 126.
(30) Kuran, P.; Krause, M.; Bartl, A.; Dunsch, L. *Chem. Phys. Lett.* **1998**, *292*, 580.
(31) Okazaki, T.; Lian, Y.; Gu, Z.; Suenaga, K.; Shinohara, H. *Chem. Phys. Lett.* **2000**, *320*, 435.
(32) Okazaki, T.; Suenaga, K.; Lian, Y. F.; Gu, Z. N.; Shinohara, H. *J. Mol. Graphics Modell.* **2001**, *19*, 244.
(33) Xu, W.; Hao, Y.; Uhlik, F.; Shi, Z.; Slanina, Z.; Feng, L. *Nanoscale* **2013**, *5*, 10409.
(34) Xu, J.; Tsuchiya, T.; Hao, C.; Shi, Z.; Wakahara, T.; Mi, W.; Gu, Z.; Akasaka, T. *Chem. Phys. Lett.* **2006**, *419*, 44.
(35) Xu, J.; Lu, X.; Zhou, X.; He, X.; Shi, Z.; Gu, Z. *Chem. Mater.* **2004**, *16*, 2959.
(36) Zheng, H.; Zhao, X.; Ren, T.; Wang, W.-W. *Nanoscale* **2012**, *4*, 4530.
(37) Feng, Y.; Wang, T.; Wu, J.; Feng, L.; Xiang, J.; Ma, Y.; Zhang, Z.; Jiang, L.; Shu, C.; Wang, C. *Nanoscale* **2013**, *5*, 6704.
(38) Gan, L.-H.; Chang, Q.; Zhao, C.; Wang, C.-R. *Chem. Phys. Lett.* **2013**, *570*, 121.
(39) Popov, A. A.; Dunsch, L. *J. Am. Chem. Soc.* **2007**, *129*, 11835.
(40) Ito, Y.; Okazaki, T.; Okubo, S.; Akachi, M.; Ohno, Y.; Mizutani, T.; Nakamura, T.; Kitaura, R.; Sugai, T.; Shinohara, H. *ACS Nano* **2007**, *1*, 456.
(41) Dewar, M. J. S.; Zoebisch, E.; Healy, E. F.; Stewart, J. J. P. *J. Am. Chem. Soc.* **1985**, *107*, 3902.
(42) Becke, A. D. *Phys. Rev. A: At., Mol., Opt. Phys.* **1998**, *38*, 3098.
(43) Becke, A. D. *J. Chem. Phys.* **1993**, *98*, 5648.
(44) Lee, C.; Yang, W.; Parr, R. G. *Phys. Rev. B: Condens. Matter Mater. Phys.* **1988**, *37*, 785.
(45) Andrae, D.; Haussermann, U.; Dolg, M.; Stoll, H.; Preuss, H. *Theor. Chim, Acta* **1990**, *77*, 123.
(46) Dolg, M.; Stoll, H.; Preuss, H. *J. Chem. Phys.* **1989**, *90*, 1730.
(47) Vlaisavljevich, B.; Miró, P.; Koballa, D.; Todorova, T. K.; Daly, S. R.; Girolami, G. S.; Cramer, C. J.; Gagliardi, L. *J. Phys. Chem. C* **2012**, *116*, 23194.
(48) Perdew, J. P.; Burke, K.; Ernzerhof, M. *Phys. Rev. Lett.* **1996**, *77*, 3865.
(49) Dolg, M.; Stoll, H.; Preuss, H.; Pitzer, R. M. *J. Phys. Chem.* **1993**, *97*, 5852.
(50) Mercado, B. Q.; Stuart, M. A.; Mackey, M. A.; Pickens, J. E.; Confait, B. S.; Stevenson, S.; Easterling, M. L.; Valencia, R.; Rodríguez-Fortea, A.; Poblet, J. M.; Olmstead, M. M.; Balch, A. L. *J. Am. Chem. Soc.* **2010**, *132*, 12098.
(51) Yang, T.; Zhao, X.; Li, S.-T.; Nagase, S. *Inorg. Chem.* **2012**, *51*, 11223.
(52) Zhang, J.; Bowles, F. L.; Bearden, D. W.; Ray, W. K.; Fuhrer, T.; Ye, Y.; Dixon, C.; Harich, K.; Helm, R. F.; Olmstead, M. M.; Balch, A. L.; Dorn, H. C. *Nat. Chem.* **2013**, *5*, 880.
(53) Frisch, M. J.; Trucks, G. W.; Schlegel, H. B.; Scuseria, G. E.; Robb, M. A.; Cheeseman, J. R.; Scalmani, G.; Barone, V.; Mennucci, B.; Petersson, G. A.; Nakatsuji, H.; Caricato,M.;Li, X.; Hratchian, H. P.; Izmaylov, A. F.; Bloino, J.; Zheng, G.; Sonnenberg, J. L.; Hada, M.; Ehara, M.; Toyota, K.; Fukuda, R.; Hasegawa, J.; Ishida, M.; Nakajima, T.; Honda, Y.; Kitao, O.; Nakai, H.; Vreven, T.; Montgomery, J. A., Jr., Peralta, J. E.; Ogliaro, F.; Bearpark,M.; Heyd, J. J.; Brothers, E.; Kudin, K. N.; Staroverov, V. N.; Kobayashi, R.;. Normand, J.; Raghavachari, K.; Rendell, A. J.; Burant, C.; Iyengar, S. S.; Tomasi, J.; Cossi, M.;

DOI: 10.1021/acs.inorgchem.5b01312
Inorg. Chem. 2015, 54, 8066−8076

Rega, N.; Millam, J. M.; Klene, M.; Knox, J. E.; Cross, J. B.; Bakken, V.; Adamo, C.; Jaramillo, J.; Gomperts, R.; Stratmann, R. E.; Yazyev, O.; Austin, A. J.; Cammi, R.; Pomelli, C.; Ochterski, J. W.; Martin, R. L.; Morokuma, K.; Zakrzewski, V. G.; Voth, G. A.; Salvador, P.; Dannenberg, J. J.; Dapprich, S.; Daniels, A. D.; Farkas, Ö.; Foresman, J. B.; Ortiz, J. V.; Cioslowski, J.; Fox, D. J. *Gaussian 09, Revision A.02*; Gaussian, Inc.: Wallingford, CT, 2009.
(54) Bader, R. F. W. *Atoms in Molecules—A Quantum Theory*; Oxford University Press: Oxford, U.K., 1990.
(55) Mayer, I. *Chem. Phys. Lett.* **1983**, *97*, 270.
(56) Mayer, I. *Int. J. Quantum Chem.* **1984**, *26*, 151.
(57) Bridgeman, A. J.; Cavigliasso, G.; Ireland, L. R.; Rothery, J. *J. Chem. Soc., Dalton Trans.* **2001**, 2095.
(58) Silvi, B.; Savin, A. *Nature* **1994**, *371*, 683.
(59) Savin, A.; Nesper, R.; Wenger, S.; Fassler, T. F. *Angew. Chem., Int. Ed. Engl.* **1997**, *36*, 1808.
(60) Kohout, M.; Wagner, F. R.; Grin, Y. *Theor. Chem. Acc.* **2002**, *108*, 150.
(61) Lu, T.; Chen, F. W. *J. Comput. Chem.* **2012**, *33*, 580.
(62) Slanina, Z.; Lee, S. L.; Uhlik, F.; Adamowicz, L.; Nagase, S. *Theor. Chem. Acc.* **2007**, *117*, 315.
(63) Yang, T.; Zhao, X.; Xu, Q.; Zheng, H.; Wang, W.-W.; Li, S.-T. *Dalton Trans.* **2012**, *41*, 5294.
(64) Chen, N.; Beavers, C. M.; Mulet-Gas, M.; Rodríguez-Fortea, A.; Munoz, E. J.; Li, Y.-Y.; Olmstead, M. M.; Balch, A. L.; Poblet, J. M.; Echegoyen, L. *J. Am. Chem. Soc.* **2012**, *134*, 7851.
(65) Stevenson, S.; Lee, H. M.; Olmstead, M. M.; Kozikowski, C.; Stevenson, P.; Balch, A. L. *Chem. - Eur. J.* **2002**, *8*, 4528.
(66) Stevenson, S.; Phillips, J. P.; Reid, J. E.; Olmstead, M. M.; Rath, S. P.; Balch, A. L. *Chem. Commun.* **2004**, 2814.
(67) Zhang, J.; Fuhrer, T.; Fu, W.; Ge, J.; Bearden, D. W.; Dallas, J.; Duchamp, J.; Walker, K.; Champion, H.; Azurmendi, H.; Harich, K.; Dorn, H. C. *J. Am. Chem. Soc.* **2012**, *134*, 8487.
(68) Yang, T.; Zhao, X. *Chem. Phys.* **2013**, *423*, 173.
(69) McAdon, M. H.; Goddard, W. A. *Phys. Rev. Lett.* **1985**, *55*, 2563.
(70) Matta, C. F.; Boyd, R. J. *The Quantum Theory of Atoms in Molecules. From Solid State to DNA and Drug Design*; Wiley-VCH: Weinheim, 2007.
(71) Jin, P.; Zhou, Z.; Hao, C.; Gao, Z.; Tan, K.; Lu, X.; Chen, Z. *Phys. Chem. Chem. Phys.* **2010**, *12*, 12442.
(72) Guo, Y.-J.; Yang, T.; Nagase, S.; Zhao, X. *Inorg. Chem.* **2014**, *53*, 2012.
(73) Guo, Y.-J.; Gao, B.-C.; Yang, T.; Nagase, S.; Zhao, X. *Phys. Chem. Chem. Phys.* **2014**, *16*, 15994.
(74) Pendas, A. M.; Blanco, M. A.; Costales, A.; Sanchez, P. M.; Luana, V. *Phys. Rev. Lett.* **1999**, *83*, 1930.
(75) Yang, T.; Zhao, X.; Xu, Q.; Zhou, C.; He, L.; Nagase, S. *J. Mater. Chem.* **2011**, *21*, 12206.
(76) Zheng, H.; Zhao, X.; Wang, W.-W.; Dang, J.-S.; Nagase, S. *J. Phys. Chem. C* **2013**, *117*, 25195.
(77) Popov, A. A. *J. Comput. Theor. Nanosci.* **2009**, *6*, 292.

DOI: 10.1021/acs.inorgchem.5b01312
Inorg. Chem. 2015, 54, 8066−8076